Tiarei inner ridge: Site M0023[1]

Expedition 310 Scientists[2]

Chapter contents

Operations 1
Sedimentology and biological assemblages . . 2
Petrophysics 3
Downhole logging 4
References 5
Figures 6

[1] Expedition 310 Scientists, 2007. Tiarei inner ridge: Site M0023. *In* Camoin, G.F., Iryu, Y., McInroy, D.B., and the Expedition 310 Scientists. *Proc. IODP,* 310: Washington, DC (Integrated Ocean Drilling Program Management International, Inc.). doi:10.2204/iodp.proc.310.107.2007
[2] **Expedition 310 Scientists' addresses.**

Operations

Hole M0023A

From 0000 h on 10 November 2005, Seacore's drilling and reentry template (DART) was raised to the moonpool after abandoning coring in Hole M0022A. The *DP Hunter* moved to a new area over a drowned reef to conduct an echo sounder survey, ~100 m southwest of proposed Site TAH-02A 4. From 0200 h on 10 November, 9 echo sounder traverses (~110 m long) were made over the drowned reef pinnacle, from which a site for Hole M0023A was chosen in 67 m water depth. After a short camera survey, coring operations in Hole M0023A started at 0635 h on 10 November and ended at 2245 h that day after reaching a total depth (TD) of 31.36 meters below seafloor (mbsf) with a total recovery of 77.20%.

Hole M0023B

After raising the DART a short distance from the seabed, the *DP Hunter* was positioned above Hole M0023B, 5 m southwest of the previous hole in 67 m water depth. Coring operations in Hole M0023B began at 0120 h on 11 November 2005 and ended at 1540 h that day at a TD of 31.12 mbsf with a total recovery of 67.90%. The coring operation proceeded smoothly, with excellent core recovery in long core runs in often very porous formation.

Prior to logging, the drill pipe was pulled and the hole flushed for 30 min before the drill pipe was run-in with a casing shoe to ~6 mbsf. Logging commenced at 1700 h on 11 November. Initially, the tools would not pass below the casing shoe, even after the chisel tool was worked in the hole. The casing shoe was run to the base of the hole and back before the chisel tool was deployed to check that the casing shoe was clear. Logging operations restarted at 2000 h, with the tools reaching a maximum depth of 28.5 mbsf. A dynamic positioning (DP) malfunction caused the vessel to move off location during the logging, but the situation was recovered and the hole and equipment remained intact. The optical and acoustic logs preview indicated that there were many cavities in the formation. Logging finished in Hole M0023B at 0310 h on 12 November.

doi:10.2204/iodp.proc.310.107.2007

Sedimentology and biological assemblages

Last deglacial sequence (Unit I)

The last deglacial sequence (lithologic Unit I) is 26 m thick in Hole M0023A, from 67.98 to 93.98 meters below sea level (mbsl), and 30 m thick in Hole M0023B, from 67.58 to 97.5 mbsl. It is primarily composed of coralgal-microbialite frameworks in which microbialites (laminated and thrombolitic microbial fabrics) usually represent the major volumetric and structural component; thrombolites usually represent the last stage of encrustation (Fig. **F1**) (e.g., interval 310-M0023A-10R-1, 66–103 cm). Primary cavities are locally partly filled with muds or with skeletal sediments comprising abundant *Halimeda* segments (Fig. **F2**) (e.g., interval 310-M0023B-4R-1, 143–151 cm), associated with mollusk and gastropod shells, and echinoid spines; volcanic silt- to sand-sized grains usually occur in those infillings, especially in the lowermost part of the sequence. Manganese(?) impregnation and dark staining of corals are reported at the top of the sequence (e.g., interval 310-M0023A-1R-1, 26 cm, and Core 310-M0023A-2R). Basalt pebbles and volcanic silt- to sand-sized grains are abundant toward the base of this sequence (Core 310-M0023A-13R).

The last deglacial sequence is characterized by three successive coral assemblages (Subunits IA–IC).

Subunit IA

Intervals: Cores 310-M0023A-1R, 3R, and 4R and 310-M0023B-1R through 5R

Subunit IA is characterized by the abundant occurrence of encrusting colonies of *Montipora*, agariciids (including *Pavona*) (Fig. **F3**) (e.g., interval 310-M0023B-3R-1, 13–36 cm), *Porites,* and *Montipora*, foliaceous colonies of *Pachyseris* associated with branching colonies of *Porites,* and, to a lesser extent, robust branching colonies of *Pocillopora.* These coral colonies display evidence of bioerosion and are usually coated by thin crusts of nongeniculate coralline algae. Fragments of branching colonies of *Pocillopora*, *Porites,* and *Acropora* also occur.

Subunit IB

Intervals: Core 310-M0023A-2R, Section 5R-1, and Core 6R

Subunit IB includes massive and encrusting colonies of *Porites* and faviids (including *Leptastrea*) (Fig. **F4**); branching colonies of *Porites* occur locally (e.g., interval 310-M0023A-2R-1, 39–47 cm). These coral colonies are extensively bored; most of the borings are still open.

Subunit IC

Intervals: Cores 310-M0023A-7R through 13R and 310-M0023B-6R through 15R

Subunit IC contains branching and encrusting colonies of *Porites* associated with encrusting colonies of *Millepora*, *Montipora, Psammocora,* and *Pavona*, massive colonies of *Leptastrea* and *Porites*, branching and robust branching colonies of *Pocillopora*, and tabular colonies of *Acropora* (Figs. **F5, F6, F7**) (e.g., intervals 310-M0023A-10R-2, 0–26 cm, 11R-1, 0–40 cm, and 13R-1, 51–71 cm). These coral colonies commonly display traces of bioerosion by bivalves. Crusts of nongeniculate coralline algae on coral colonies are usually thin, except in some intervals where they are well developed in association with vermetid gastropods and serpulids (Cores 310-M0023A-13R and 310-M0023B-6R, 8R, and 10R). Branching *Porites* frameworks are locally fragmented to form rudstone intervals (Cores 310-M0023B-5R and 6R). Coralgal-microbialite frameworks are locally interlayered with beds of rubble composed of branching *Porites* and *Pocillopora* fragments and *Halimeda* segments (e.g., Core 310-M0023B-15R).

Older Pleistocene sequence (Unit II)

Intervals: Cores 310-M0023A-14R through 16R and 310-M0023B-16R

The older Pleistocene sequence (lithologic Unit II) is composed of brown well-lithified algal bindstone, microbialites, and coralgal frameworks that exhibit evidence of diagenetic alteration, including the transformation of coral skeletons and the occurrence of solution cavities. The matrix of the coralgal frameworks is composed chiefly of silt to fine sand-sized skeletal grains (Fig. **F8**) (e.g., interval 310-M0023A-14R-1, 68–87 cm). Basalt pebbles and lithoclasts occur throughout this sequence. Core 310-M0023B-15R recovered coral clasts derived from robust branching colonies of *Pocillopora* and branching colonies of *Porites*, which display traces of diagenetic alteration. Solution cavities occur throughout this interval and are filled with several generations of infillings, including well-lithified, pale brownish limestone and poorly lithified dark brown sandy sediments, including skeletal grains.

The coral assemblage includes massive and encrusting colonies of faviids (including *Montastrea*) (Fig. **F9**), robust branching and tabular colonies of *Acropora,* encrusting colonies of agariciids, and branching colonies of *Porites* (e.g., interval 310-M0023A-15R-1, 17–37 cm). Fragmented coral colonies include branching *Pocillopora* and *Porites* and tabular *Acropora*.

Petrophysics

Recovery at Tiarei inner ridge Site M0023, on the northeastern side of the island of Tahiti, was generally good (Hole M0023A = 77%; Fig. **F10**). Good recovery is mainly from the last deglacial sequence (Unit I). The older Pleistocene sequence (Unit II) has discontinuous (Hole M0023A; Fig. **F10**) to no data (Hole M0023B; Fig. **F11**). Cores 310-M0023A-14R, 15R, 16R, and 16R were left unsaturated and therefore have different data coverage and quality (see the **"Methods"** chapter for more details). Water depths are as follows: Hole M0023A = 67.98 mbsl and Hole M0023B = 67.58 mbsl.

Density and porosity

Bulk density at Tiarei inner ridge sites was computed from gamma ray attenuation (GRA) and moisture and density (MAD) measurements on discrete plug samples. In both holes, three intervals are recognized.

- Interval 1 corresponds to the top of the last deglacial sequence, from 0 to 11 mbsf (Cores 310-M0023A-1R through 7R). This interval shows a scattered, generally low density of ~2.0 g/cm^3. Porosity is as high as 50% but is generally ~35%–40%.
- Interval 2 (Cores 310-M0023A-8R through 13R) is also located in the last deglacial sequence. The upper boundary (11 mbsf) shows a remarkable sharp change in density and porosity and coincides with a change in coral assemblages (see **"Sedimentology and biological assemblages"**). Densities are higher, ~2.2 g/cm^3, and average porosity is ~30%. Toward the lower part of this unit, recovery drops and a slight decrease in density is observed.
- Interval 3 (24.5 mbsf to the bottom of the hole; Cores 310-M0023A-14R through 16R) corresponds to the older Pleistocene sequence and has poor recovery because of poor lithification. Sediments consist of coral gravels with densities of ~2.3 g/cm^3 and highly scattered porosity values ranging from 15% to 30% with outliers to 50%. MAD density ranges between 1.84 and 2.64 g/cm^3 for Unit I and increases to 2.69 to 2.80 g/cm^3 for Unit II (e.g., 26 mbsf in Hole M0025A).

Grain density values average 2.77 g/cm^3, range between 2.69 and 2.81 g/cm^3, and do not show any clear downhole trends. Average grain density is not consistent with calcite mineralogy (2.71 g/cm^3). It is thought that deviations occur because of the volcaniclastic input for which minerals have different matrix densities.

P-wave velocity

P-wave velocities were measured with the Geotek MSCL *P*-wave logger (PWL) on whole cores and the PWS3 contact sensor system on a modified Hamilton frame on ~2–4 cm long, 1 inch round discrete samples of semilithified and lithified sediments (see the **"Methods"** chapter). Velocities in one transverse (x) direction were measured on the plugs. Velocities follow the same subdivision into three intervals, as described in **"Density and porosity."** Interval 1 shows scattered observations around 3000 m/s with slower velocities centered around 1800 m/s. Simultaneously with the increase in density in Interval 2, the velocity profile is more continuous with an average velocity of 3900 m/s. Toward the lower part of Interval 2, density decreases slightly, and velocities follow this trend toward 3600 m/s. Interval 3 does not reveal any velocity measurements, as sections from this depth were left unsaturated because of the presence of (semi-) lithified gravels and sands.

Measurements on discrete samples confirm velocities measured with the MSCL. Discrete velocity measurements range from 3781 to 4830 m/s and generally represent the higher velocities observed in core measurements. A cross plot of velocity versus porosity for Tiarei inner ridge sites reveals a general inverse relationship (Fig. **F12**). For the time-average empirical equation of Wyllie et al. (1956) and Raymer et al. (1980), the traveltime of an acoustic signal through rock is a specific sum of the traveltime through the solid matrix and the fluid phase. Porosity and velocity data do not match the time-average equation but show large scatter around the general trend line. For a given density of 2.0 g/cm^3, velocity may vary as much as 2000 m/s. Comparison of V_P MSCL data and downhole sonic logging data (Fig. **F13**) confirms scattered velocity data. Peaks in high velocity values correlate well. Sonic logging values are on average 500 m/s slower than V_P MST, attributable to scaling effects. Whereas the MSCL measures velocity directly only on matrix sediments, the sonic log provides an average over an interval of 1 ft (~31 cm) in which velocity is averaged over large primary pores containing seawater (~1535 m/s) and rock, always resulting in a lower average than direct measurements of matrix properties.

Magnetic susceptibility

Magnetic susceptibility at this site also follows the general subdivision into intervals (see **"Density and porosity"**). Interval 1 has highly variable magnetic susceptibilities varying from 0 to a maximum of 600 × 10^{-5} SI units. Susceptibilities vary over short distances, and individual peaks from locations associated with a high influx of volcaniclastics correlate

with the higher values. Interval 2 reveals a highly variable but generally high level of magnetic susceptibility. Values on average lie around 500 × 10^{-5} SI units with lower limits around 300 × 10^{-5} SI units and maxima up to 750 × 10^{-5} SI units. Zone 3 has lower magnetic susceptibilities with a maximum of 220 × 10^{-5} SI units but averages ~120 × 10^{-5} SI units. High susceptibility values may be associated with a higher concentration of magnetic minerals because of the proximal location of the Tiarei River, which brings in a high influx of generally fine to coarse sand-size volcaniclastic material.

Resistivity

See **"Resistivity"** in the "Maraa western transect" chapter.

Diffuse color reflectance spectrophotometry

In the last deglacial sequence at Site M0023, color reflectance values range from 25 to 79 L* units (Fig. **F14**). No clear downhole trends can be observed in Hole M0023B. Highest values of L* in Unit I (up to 79 L* units) originate from measurements on massive *Porites* corals in Sections 310-M0023A-5R-1 and 6R-1 (6.7–9.9 mbsf). In Unit II (Cores 310-M0023A-15R through 16R; below 27.4 mbsf), color reflectance again has L* values up to 79 L* units. This interval corresponds to the coralgal framework that includes *Acropora, Porites,* and faviid corals.

Hole-to-hole correlation

Holes M0023A and M0023B are located several meters away from each other. Clear correlation of Intervals 1 and 2 is made based on density and magnetic susceptibility changes (Fig. **F15**).

Downhole logging

Hole M0023B

Hole M0023B (67.58 mbsl) was logged for geophysical parameters. Drilling depth was 30.12 mbsf, and geophysical wireline operations were completed from 28.97 mbsf upward with data coverage from all slimhole tools without repositioning the open shoe casing (fixed at 4.63 mbsf) under open and very hostile borehole conditions. The superb quality of the image logs allows clear identification of lithologies forming eight distinct intervals:

- Interval 1 (9.22–28.97 mbsf; Cores 310-M0023B-12R through 15R) contains relatively high natural radioactivity where elements Th and K contribute most to the total counts measured (Fig. **F16**). The quality of the optical images of the lowermost 3 m is affected by murky borehole fluids and enlarged borehole diameter. From 25.90 mbsf, in situ open frameworks composed of branching coral colonies can be observed in borehole wall images. The minimum in total counts at 24.42 mbsf correlates with the occurrence of a branching colony of *Porites,* as observed in the optical image. At 23.62 mbsf, a (sharp) change from branching colonies to more encrusting coral growth forms (*Porites* and faviids) occurs. Resistivity values were very low (~1.65 m), the temperature of the borehole fluid was ~27.2°C, pH values were ~7.92, and electrical conductivity increased from 56.09 to 56.64 mS/cm (0.1765–0.1783 m). Sonic *P*-wave velocities (V_P) decreased from 2418 to 1709 m/s from base to top in the second sequence. Proper sonic Stoneley wave velocities could not be measured.
- Interval 2 (20.81–23.00 mbsf; Core 310-M0023B-11R) is characterized by a local total counts maximum in the gamma ray log at 22.9 mbsf that can be correlated with a very large borehole diameter and a thin sand interval with fragments of coralgal material just above. It shows an increase in resistivity from 1.22 to 2.47 Ωm, an increase in V_P from 1709 to 3456 m/s, and a decrease in natural radioactivity (Fig. **F16**). The temperature of the borehole fluid was ~27.37°C, pH values were ~7.95, and electrical conductivity increased from ~56.71 mS/cm (0.176 Ωm).
- Interval 3 (18.51–20.81 mbsf; Core 310-M0023B-10R) has a top-bounding surface marked by a relatively thick algal crust. Some less pronounced surfaces are present within this section (e.g., erosional contact between a thin-branching coral colony and an interval consisting of coral fragments at 19.43 mbsf). Resistivity increased slightly from 2.11 to 2.65 Ωm, V_P increased at the base from 2382 to 3456 m/s but became highly variable toward the top, gamma radiation decreased, and borehole fluid properties remained constant. In the middle part of the last deglacial sequence (13.93–18.51 mbsf; Cores 310-M0023B-8R and 9R), formation resistivity increased over a couple of steps from 2.23 Ωm to a maximum of 3.9 Ωm. These steps can be correlated with lithological changes.
- Interval 4 (17.50–18.51 mbsf; Core 310-M0023B-8R) shows coral fragments on top of an encrusted surface just below a cavity (Fig. **F17**). A marked difference in the thickness of the coral branches can be observed when comparing this lithofacies with the same lithofacies in the section below. Furthermore, a marked increase in the intensity of microbialite encrusting can be observed with

higher amplitude values in the acoustic borehole image (ABI40) and directly in the optical borehole image (OBI40). Upsection, the coral framework becomes more open, coral branches become thinner, and microbialite encrusting is less intensive. At the very top, some thinly encrusting corals can be observed. Within this interval, V_P decreased from 3314 to 2166 m/s.

- Interval 5 (13.93–17.50; Cores 310-M0023B-8R and 9R) comprises rubble in which a pinkish/orange-colored fragment of *Pocillopora* can be observed on the color-calibrated optical image at 17.25 mbsf (Fig. **F17**). Branching coral colonies are dominated by *Pocillopora* in the lower part, and the volumetric contribution of microbialite is >50%. Microbialite encrusting remains very abundant upsection, resulting in the highest formation resistivity values in Hole M0023B. A subtle increase in borehole fluid pH values occurred along with a decrease in fluid conductivity and fluid temperature within this subsequence (14.55 mbsf). The upper part of Hole M0023B displayed a decrease in resistivity to a minimum of 1.3 Ωm at 9.10 mbsf; below that point, resistivity remained fairly constant at ~2.1 Ωm.
- Interval 6 (11.69–13.93 mbsf; Core 310-M0023B-7R) contains intervals of nearly homogeneous microbialite encrustations up to 25 cm thick (e.g., 12.88–13.93 mbsf). Branching colonies of corals also occur, and from 12.11 mbsf the topmost horizon consists mainly of foliaceous corals encrusted by microbialite crusts. The uppermost 45 cm consists of less massive coral assemblages with a more open framework and less pronounced microbialite encrustation. Formation resistivity decreased in this upper interval (Fig. **F16**).
- Interval 7 (9.22–11.69 mbsf; Cores 310-M0023B-6R and 7R) consists of branching and more massive coral assemblages, where a decrease in the thickness of branches and in microbialite encrusting can be observed upsection. V_P data coverage is not optimal, but a general decrease (3566–1567 m/s) in V_P can be observed.
- Interval 8 (4.63–9.22 mbsf; Cores 310-M0023B-3R through 5R) contains two cavities at the base. Above these, an interval of very open framework composed of branching, foliaceous, and encrusting coral assemblages can be observed. The abundance of microbialite encrustations decreases upsection.

References

Raymer, L.L., Hunt, E.R., and Gardner, J.S., 1980. An improved sonic transit time-to-porosity transform. *Trans. SPWLA 21st Annu. Log. Symp.,* Pap. P.

Wyllie, M.R.J., Gregory, A.R., and Gardner, L.W., 1956. Elastic wave velocities in heterogeneous and porous media. *Geophysics,* 21(1):41–70. **doi:10.1190/1.1438217**

Publication: 4 March 2007
MS 310-107

Figure F1. Coralgal-microbialite framework composed of branching *Porites* colonies, coralline algal crusts, and massive laminated to thrombolitic microbialite masses (Subunit IC; interval 310-M0023A-10R-1, 66–103 cm).

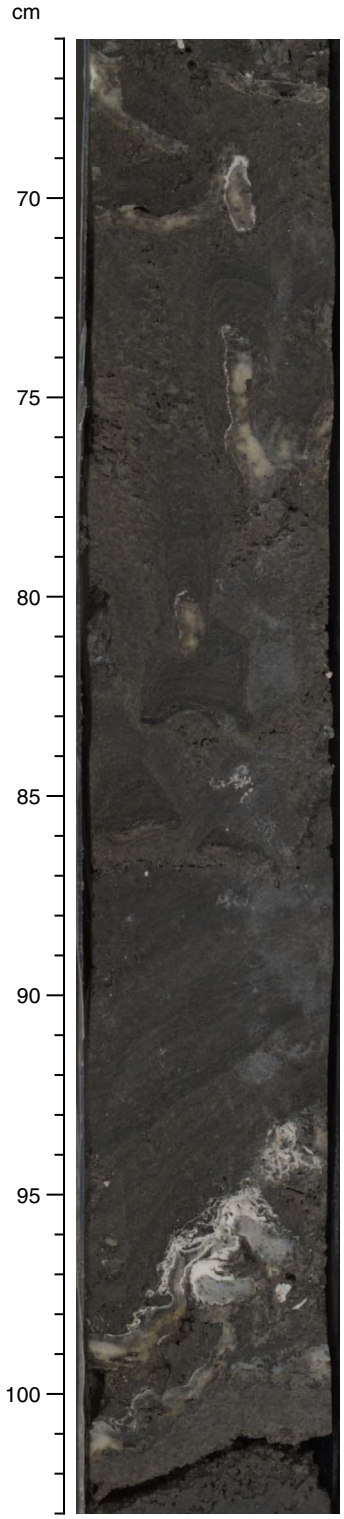

Figure F2. Coralgal bindstone with cavities filled with *Halimeda*-rich sediment (Unit I; interval 310-M0023B-4R-1, 143–152 cm).

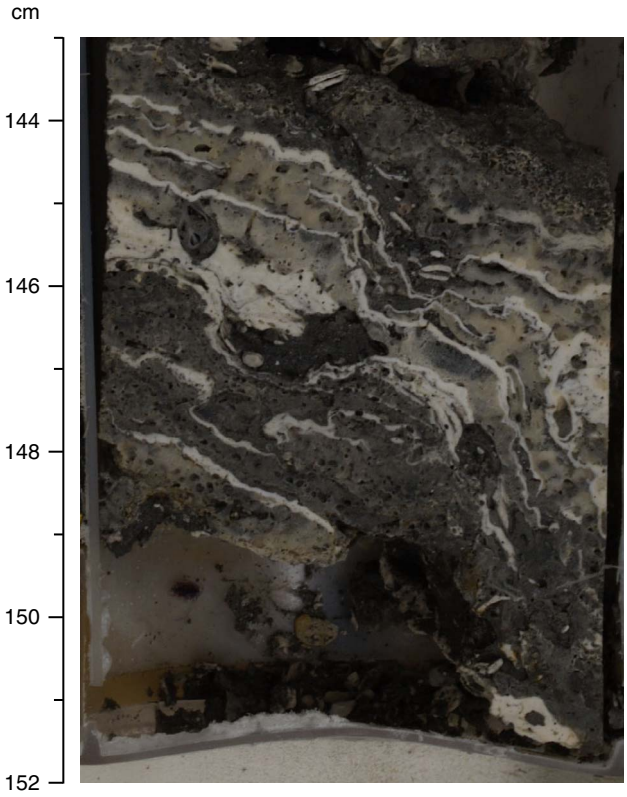

Figure F3. Encrusting colonies of agariciids interlayered with coralline algal crusts (Subunit IA; interval 310-M0023B-3R-1, 13–36 cm).

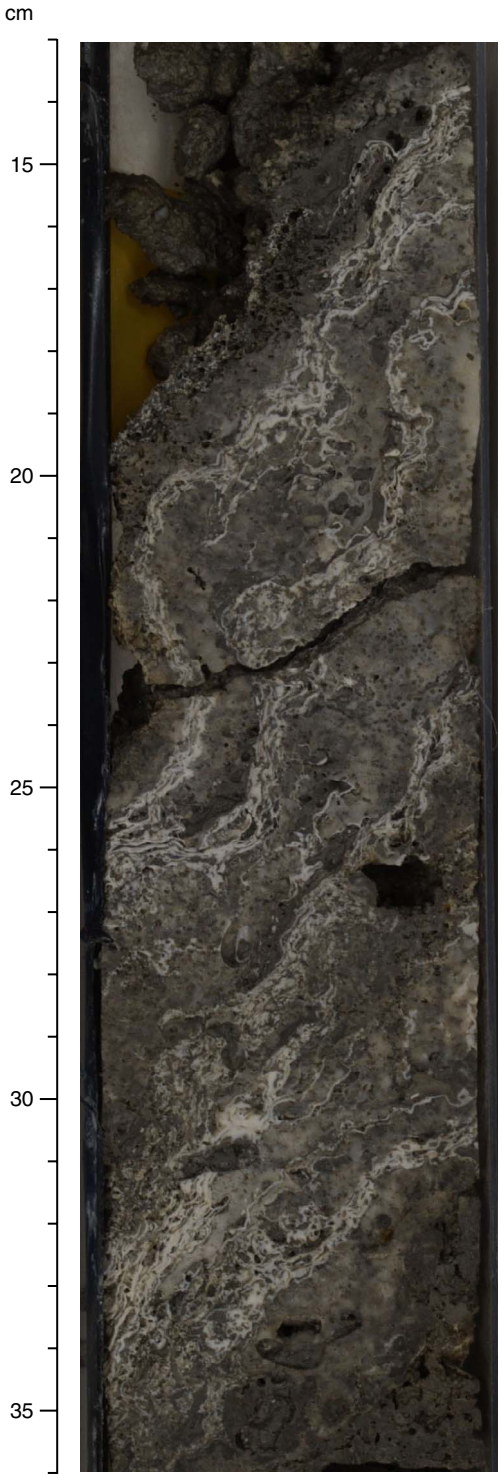

Figure F4. Massive and encrusting colonies of *Porites* and *Leptastrea* coated by thin coralline algal crusts (Subunit IB; interval 310-M0023A-2R-1, 29–44 cm). Note extensive bioerosion in corals.

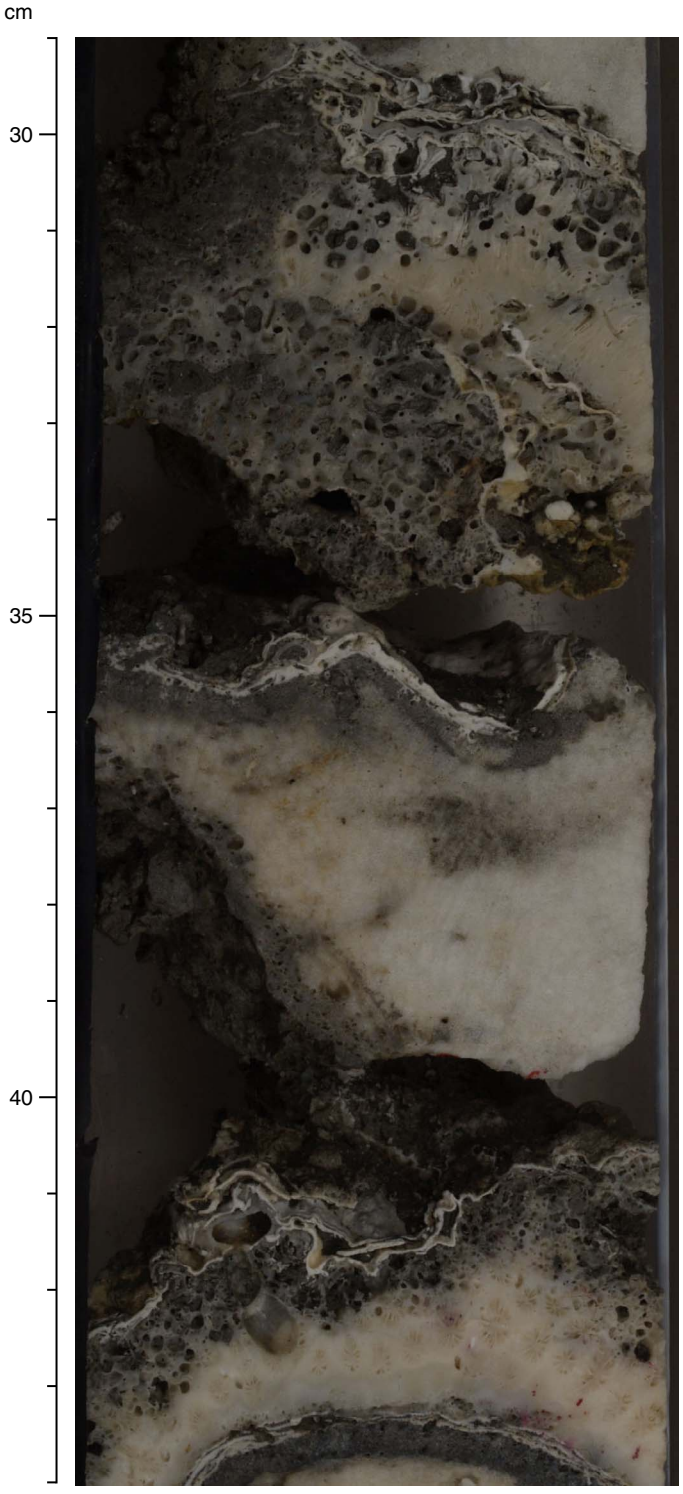

Figure F5. Coralgal microbialite framework composed of branching *Porites* colonies and massive microbialite masses (Subunit IC; interval 310-M0023A-10R-2, 0–26 cm). Note the occurrence of skeletal sand bearing *Halimeda* segments.

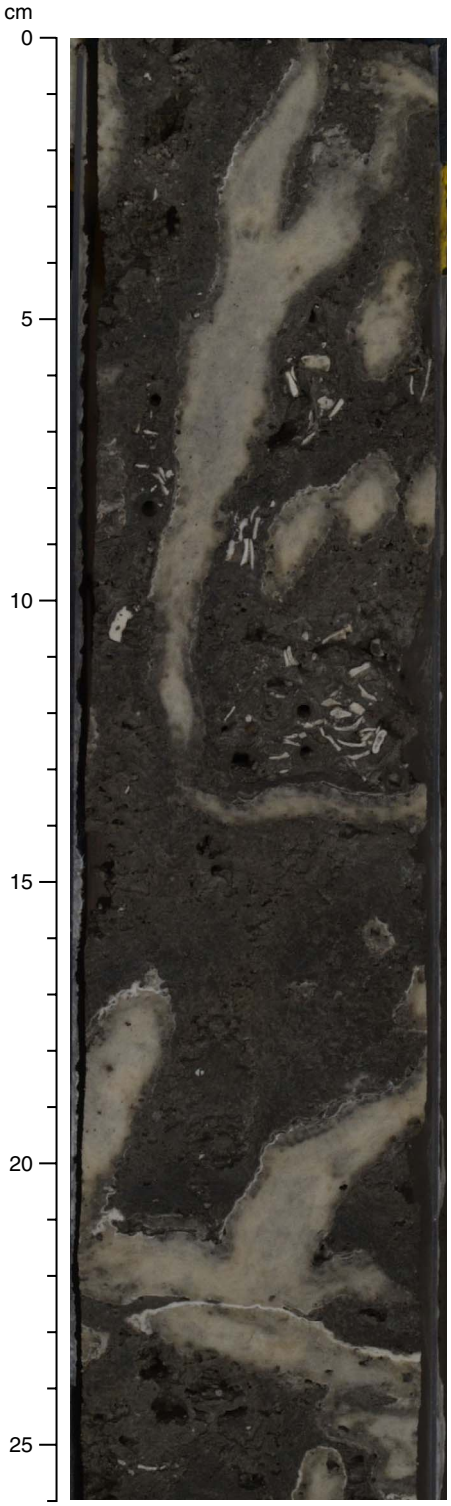

Figure F6. Robust branching *Pocillopora* framework (Subunit IC; interval 310-M0023A-11R-1, 1–40 cm). Note the occurrence of skeletal sand with *Halimeda* segments between coral colonies.

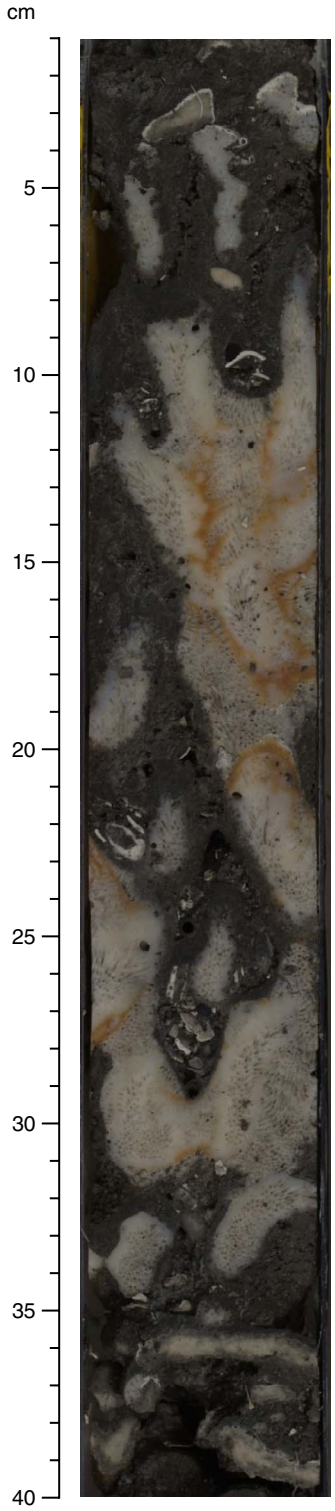

Figure F7. Coralgal framework with tips of robust branching *Pocillopora* encrusted by coralline algae and subsequent encrusting *Porites* (Subunit IC; interval 310-M0023A-13R-1, 51–72 cm). Note bioerosion affecting coral colonies.

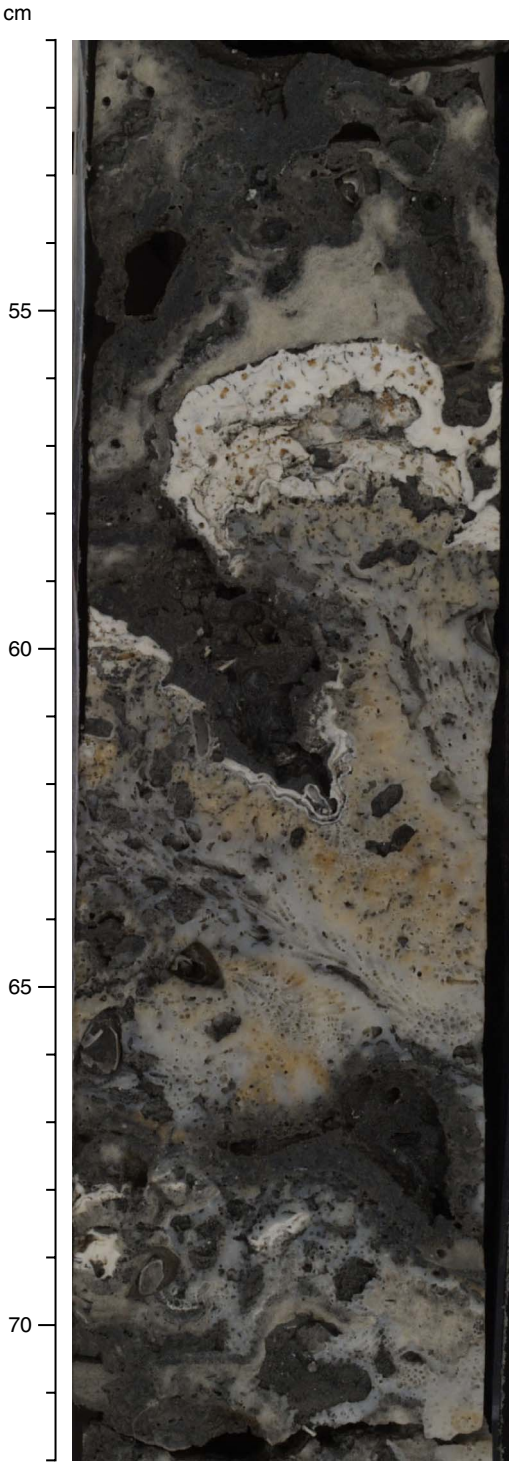

Figure F8. Multiple generations of thin coralline algal crusts encrusted by thick microbialite masses primarily composed of columnar accretions (Unit II; interval 310-M0023A-14R-1, 67–87 cm).

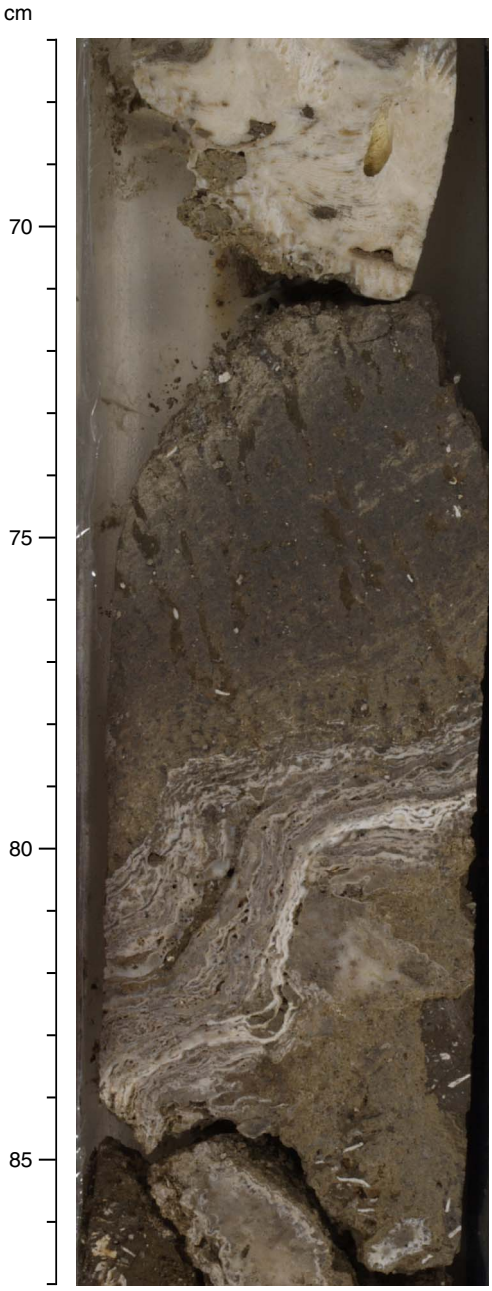

Figure F9. Massive colonies of *Montastrea* from the older Pleistocene sequence (Unit II; interval 310-M0023A-15R-1, 17–34 cm).

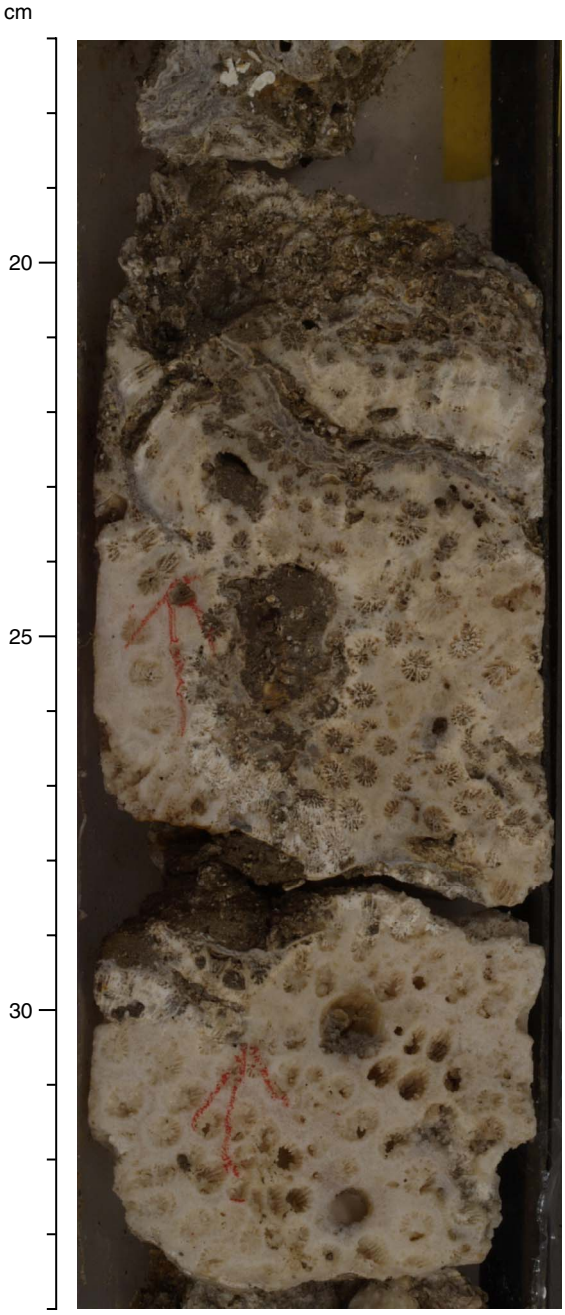

Figure F10. Velocity, bulk density, magnetic susceptibility, and porosity as a function of depth in Hole M0023A. Discrete measurements are superimposed (red circles).

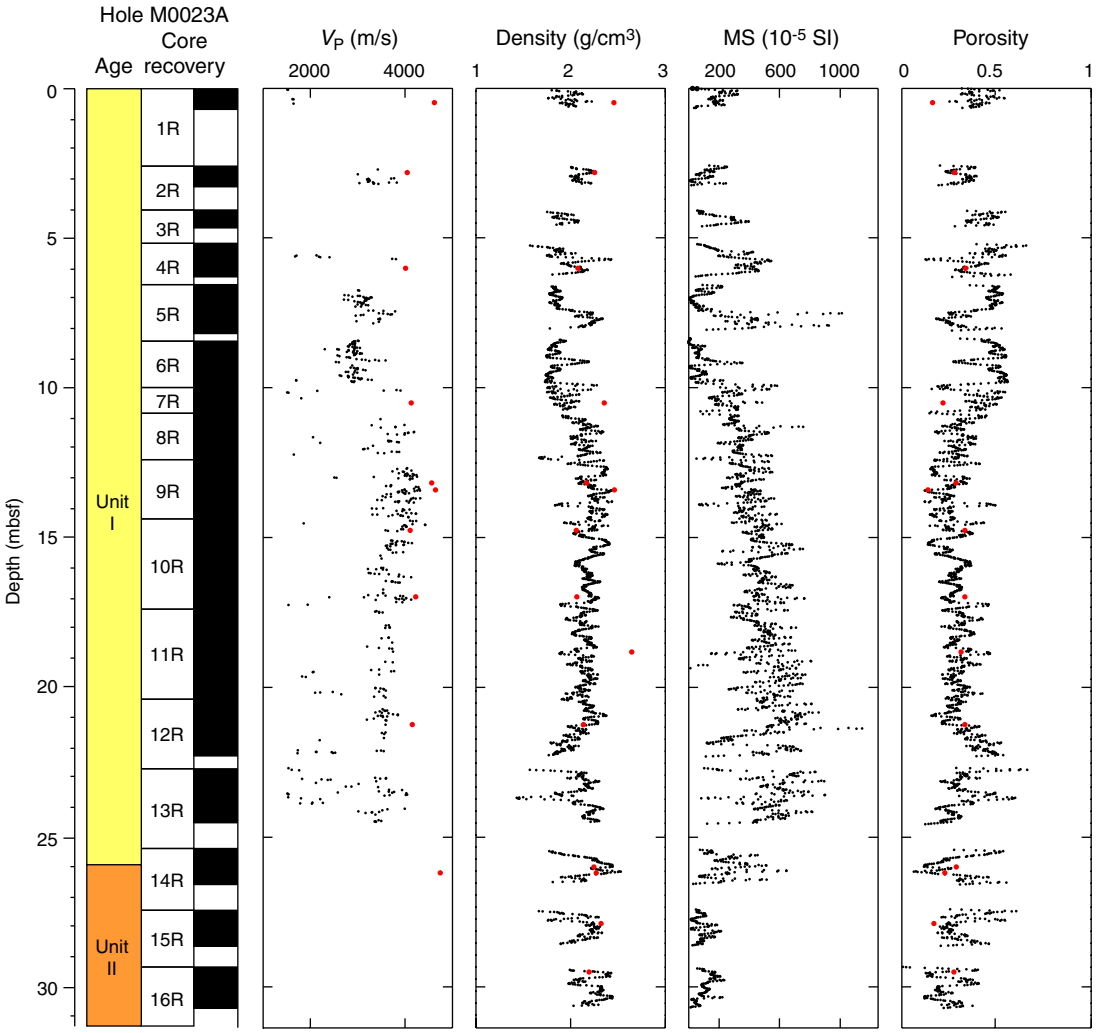

Figure F11. Velocity, bulk density, magnetic susceptibility, and porosity as a function of depth in Hole M0023B. Discrete measurements are superimposed (red circles).

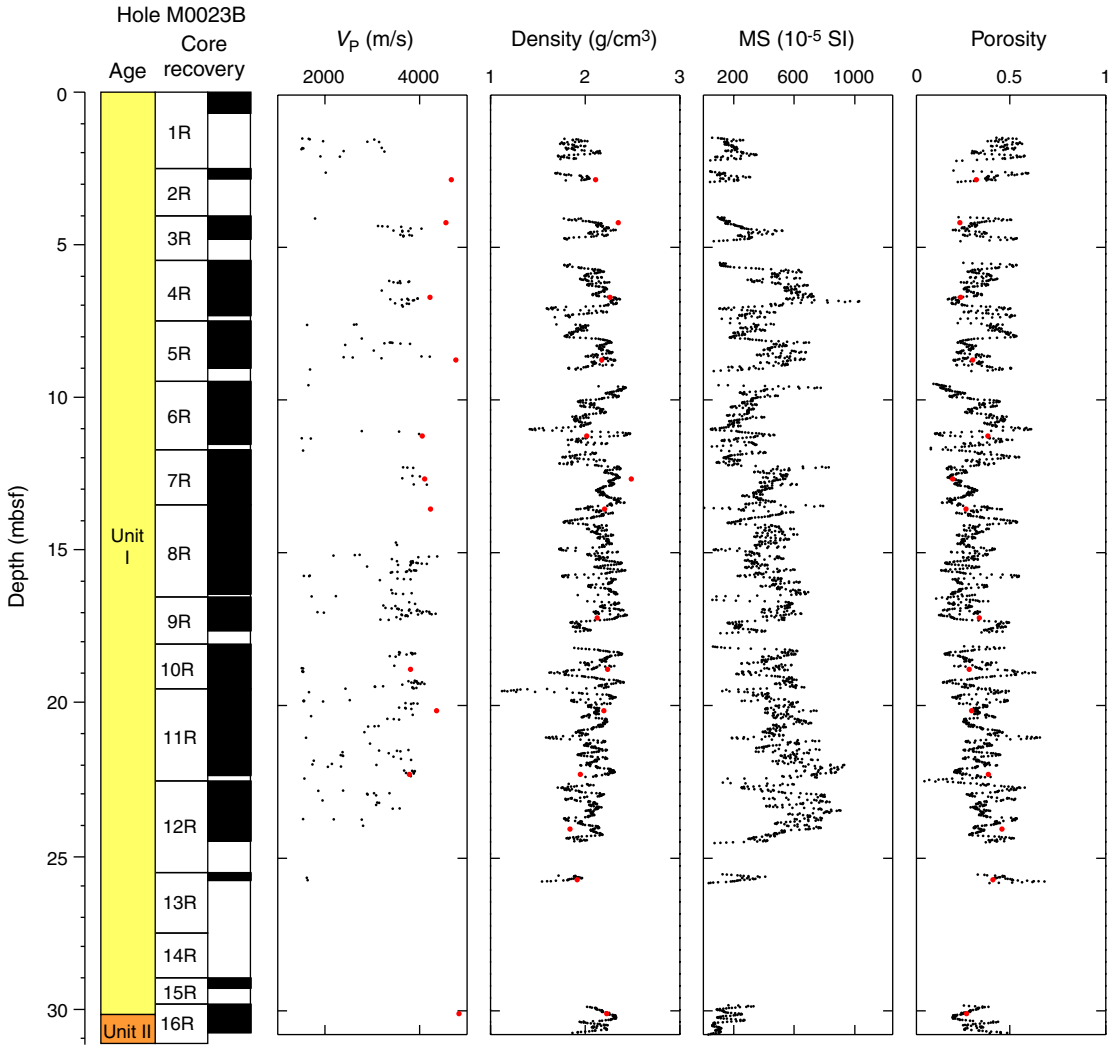

Figure F12. Cross plot of porosity with velocity for Hole M0023A. Solid lines refer to the Wyllie time average equation (red) and Raymer modified time average equation (green) for a matrix velocity of calcite (6530 m/s). Discrete measurements are superimposed (red circles).

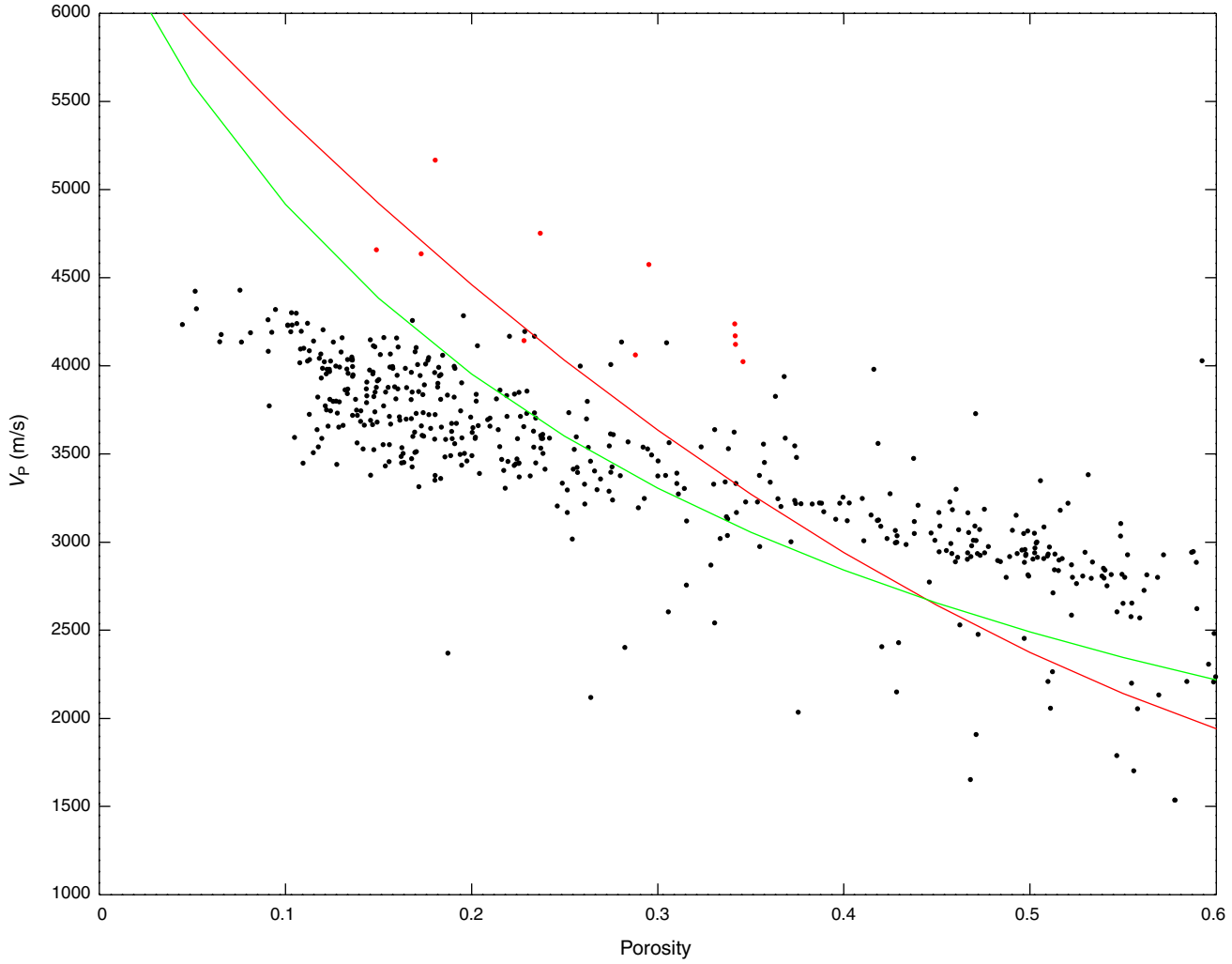

Figure F13. Comparison of MSCL velocity data (black circles), downhole sonic log data (blue line), and discrete measurements (red circles) as a function of depth for Hole M00023B.

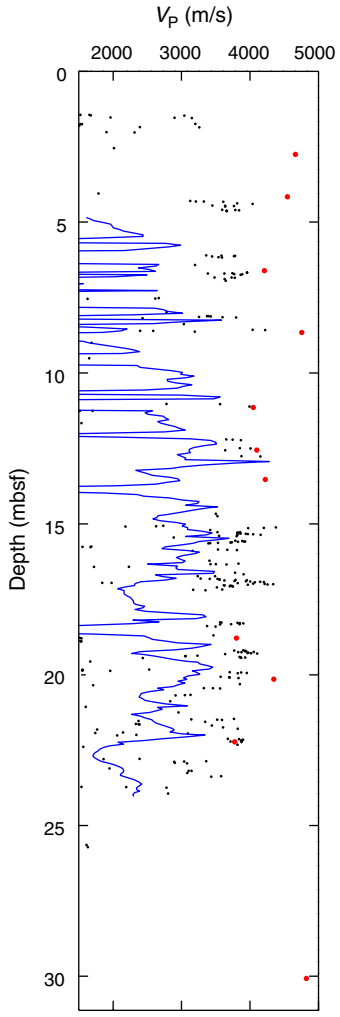

Figure F14. Color reflectance (L*) data from Holes M0023A and M0023B. For plotting purposes, Hole M0023B is offset from Hole M0023A by 50 L* unit.

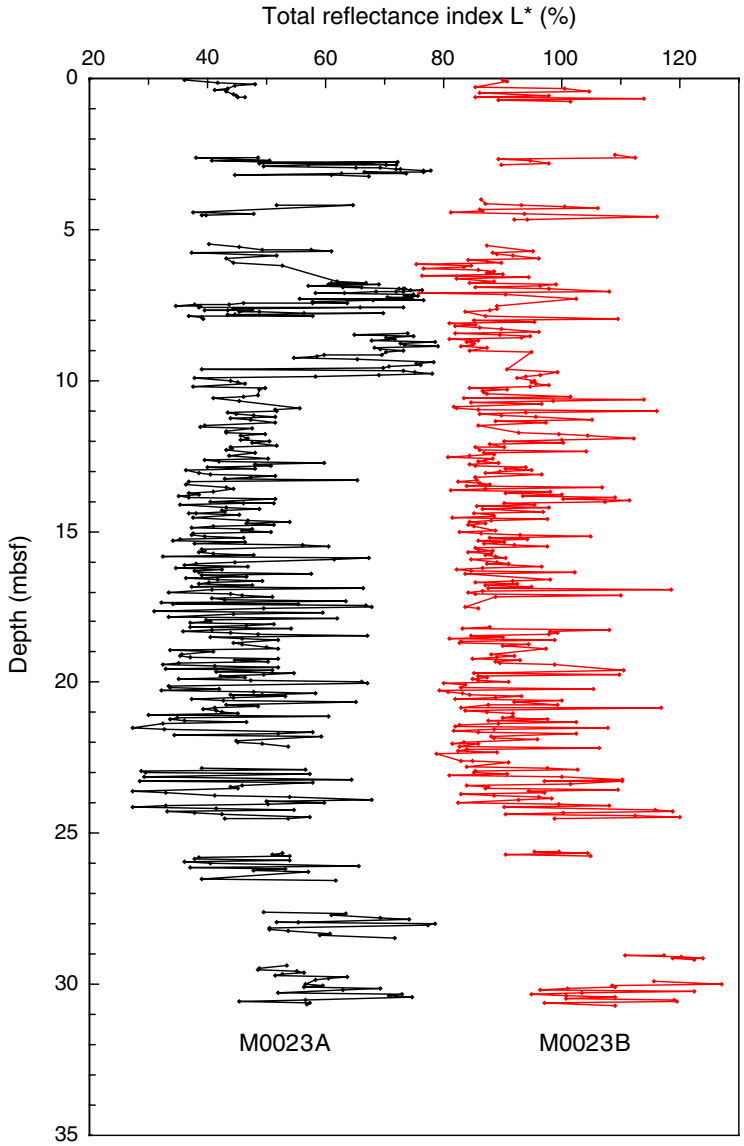

Figure F15. MSCL density and magnetic susceptibility correlation diagram as a function of depth for Site M0023.

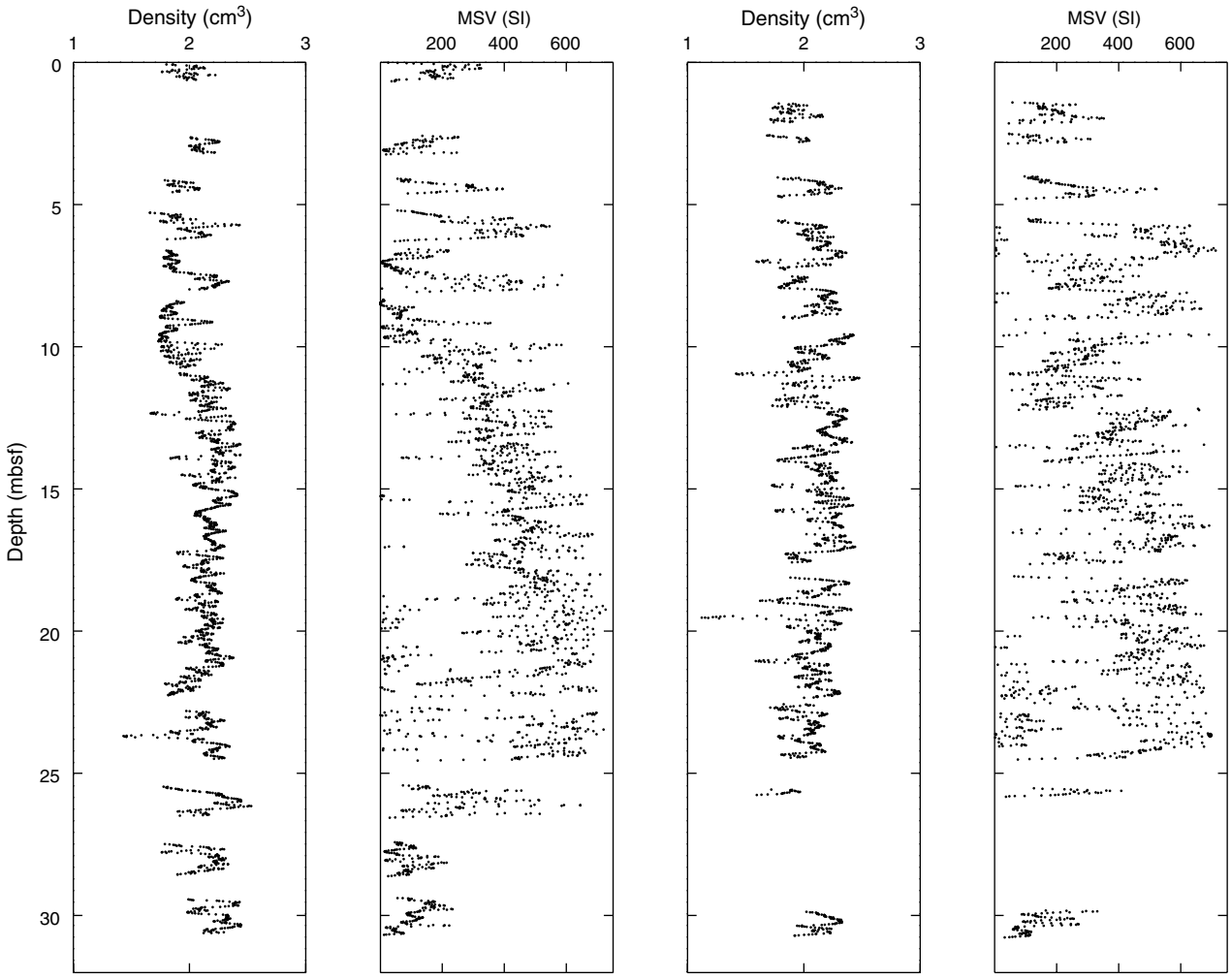

Figure F16. Wireline logging data, Hole M0023B. Ac. cal. = acoustic caliper derived from ABI40, Mec. cal. = mechanical caliper, TGR = total gamma ray, res. = resistivity, T = borehole fluid temperature, C = borehole fluid conductivity.

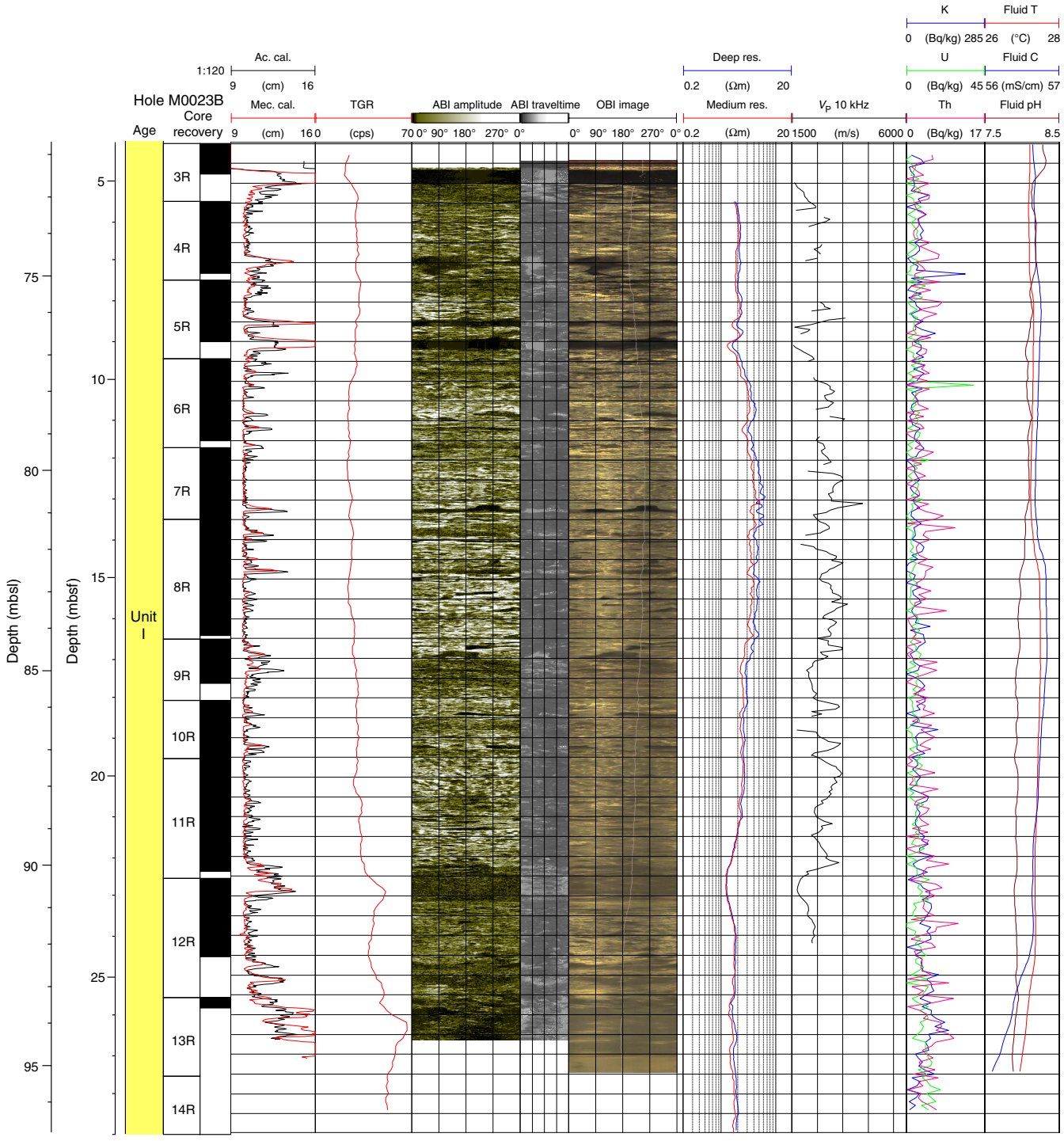

Figure F17. Wireline logging data, Hole M0023B. Ac. cal. = acoustic caliper derived from ABI40, Mec. cal. = mechanical caliper. (See the "DOWNHOLE" folder in **"Supplementary Material"** for the complete multipart figure in PDF format.)